Siliconix

A Commutation Double-Balanced MOSFET Mixer of High Dynamic Range

Ed Oxner
January 1986
Siliconix incorporated

INTRODUCTION

Dynamic range remains the principle goal of high-frequency (HF) mixer designs. The intermodulation performance and overload characteristics of a mixer are fundamental qualities used in the evaluation of a good design.

Heretofore, most mixers sporting a high dynamic range have been either the passive diode-ring variety – available from numerous vendors – or the active FET mixer. The latter is often implemented, using either the Siliconix U310 or the Siliconix U350, from earlier published design notes (1)(2).

Common to both the diode and FET is their square-law characteristic so important in maintaining low distortion during mixing. However, equally important for high dynamic range is the ability to withstand overload that has been identified as a principle cause of distortion in mixing (3). Some passive diode-ring mixer designs have resorted to paralleling of diodes to effect greater current handling, yet the penalty for this apparent improvement is the need for a massive increase in local-oscillator power.

This report examines a new FET mixer where commutation achieves high dynamic range without exacting the anticipated penalty of increased local-oscillator drive. Using the Siliconix Si8901 monolithic quad-ring small-signal double-diffused MOSFET, third-order intercept points upward of +39 dBm (input) have been achieved with only +17 dBm of local-oscillator drive. A comparison between the Si8901 double-balanced mixer and the conventional diode ring double-balanced mixer is offered in Figure 1 where we see an order-of-magnitude improvement in performance at-local-oscillator power levels substantially lower than heretofore possible with the conventional mixer.

CONVERSION EFFICIENCY OF THE COMMUTATION MIXER

Unlike either the conventional diode-ring mixer or the active FET mixer, the commutation mixer relies on the switching action of the quad-FET elements to effect mixing action. Consequently, the commutation mixer is, in effect, no more than a pair of switches reversing the phase of the signal carrier at a rate determined by the local-oscillator frequency. Ideally, we would anticipate little noise contribution, and since the switching mixer – consisting of four MOSFET "switches" – has finite ON-state resistance, performance is similar to that of a switching attentuator. As a result, the conversion efficiency of the commutation mixer may be expressed as a loss.

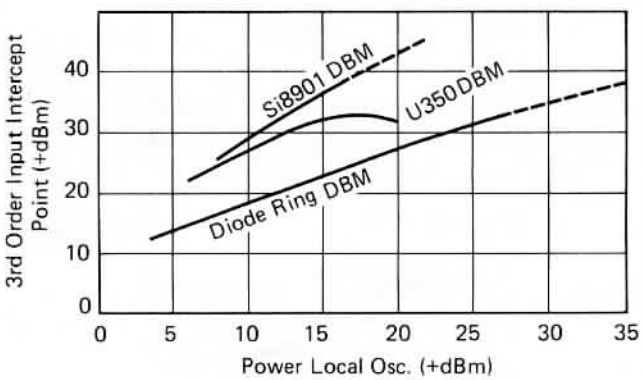

Performance Comparison of Double Balanced Mixers

Figure 1

This loss results from two related factors. First, is the r_{DS} of the MOSFET relative to the signal impedance (R_g) and intermediate frequency (IF) impedance (R_L); second – and a more common and expected factor – is the loss attributed to signal conversion to undesired frequencies. The latter signal conversion involves the image and harmonic frequencies. There are, however, ways to reduce the effects of undesired frequency generation by filtering.

The effect of r_{DS} of the MOSFETs may be determined from the analysis of the equivalent circuit shown in Figure 2, assuming that our local oscillator waveform is an idealized square wave. It is not, but if we assume that it is, our analysis is greatly simplified; and for a commutation mixer, a high local-oscillator voltage begins to approach the ideal waveform of a square wave.

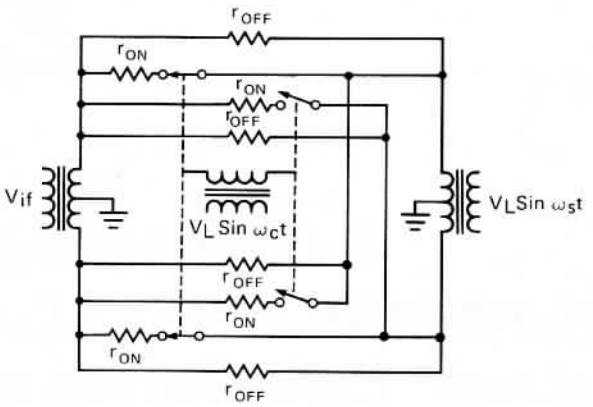

Equivalent Circuit of Communication Mixer

Figure 2

Figure 2, showing switches rather than MOSFETs, also identifies the ON-state resistance, r_{DS}, as well as the OFF-state resistance, r_{OFF}. The latter can be disregarded in this analysis as it is generally extremely high ($> 2 \cdot 10^{9}\ \Omega$). On the other hand, the ON-state resistance, r_{DS}, together with the source and load impedances (i.e., signal and intermediate-frequence impedances) directly affects the conversion efficiency.

If we assume that our local-oscillator excitation is an idealized square wave, the switching action may be represented by the Fourier series as,

$$f(x) = \frac{1}{2} + \frac{2}{\pi} \sum_{n=1}^{\infty} \frac{\sin(2n-1)\,\omega t}{(2n-)} \quad \ldots \qquad (1)$$

The switching function, ϵ (t), shown in the derivative equivalent circuit of Figure 3, is derived from the magnitude of this Fourier series expansion as a *power* function by squaring the first term, i.e. $(2/\pi)^2$.

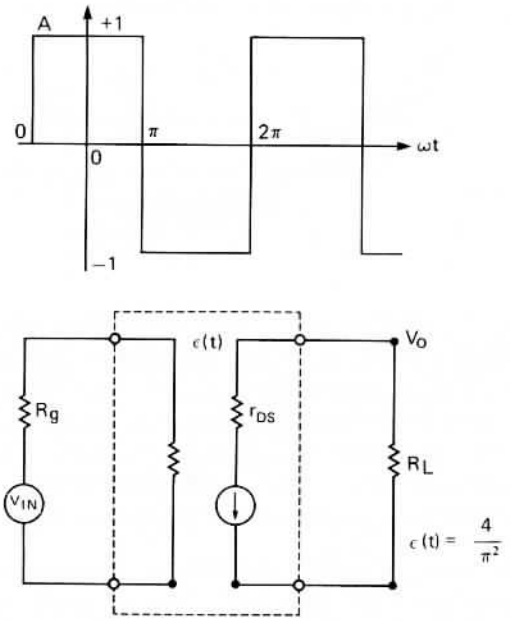

Derivative Equivalent Circuit

Figure 3

The available power that can be delivered from a generator of RMS open-circuit terminal voltage, V_{in}, and internal resistance, R_g, is

$$P_{av} = \frac{V_{in}^2}{4R_g} \qquad (2)$$

or, in terms shown in Figure 4,

$$P_{av} = \frac{V_{in}^2}{\pi^2 R_g} \qquad (3)$$

the output power, deliverable to the intermediate-frequency port, is

$$P_{out} = \frac{V_o^2}{R_L} \qquad (4)$$

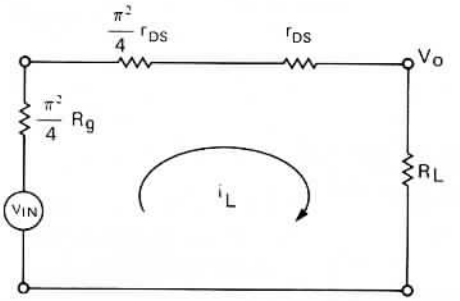

The Power-Loop Circuit with All Elements Equivalent Based on the Transfer Function, $\epsilon(t) = \frac{4}{\pi^2}$

Figure 4

To arrive at V_o, we first need to obtain the loop current, i_L, which from Figure 4 offers

$$i_L = \frac{V_{in}}{\frac{\pi^2}{4}(R_g + r_{DS}) + R_L + r_{DS}} \qquad (5)$$

then

$$V_o = \frac{V_{in} R_L}{\frac{\pi^2}{4}(R_g + r_{DS}) + R_L + r_{DS}} \qquad (6)$$

Combining Equations (4) and (6),

$$P_{out} = \frac{V_{in}^2 R_L}{\left[\frac{\pi^2}{4}(R_g + r_{DS}) + R_L + r_{DS}\right]^2} \qquad (7)$$

Conversion efficiency – in the case for the commutation mixer, a loss – may be calculated from the ratio of P_{av} and P_{out}

$$L_c = 10 \operatorname{Log} \frac{P_{av}}{P_{out}} \ \text{dB} \qquad (8)$$

Substituting Equation (3) for P_{av}, and Equation (7) for P_{out}, we obtain

$$L_c = 10 \operatorname{Log} \frac{\left[\frac{\pi^2}{4}(R_g + r_{DS}) + R_L + r_{DS}\right]^2}{\pi^2 R_L R_g} \ \text{dB} \qquad (9)$$

The conversion loss represented by Equation (9) is for a broadband double-balanced mixer with all ports matched to the characteristic line impedances. The ideal commutating mixer operating with resistive source and load impedances will result in having the image and all harmonic frequencies dissipated. For this case, the optimum conversion loss reduces to

$$L_c = 10 \text{ Log } \frac{4}{\pi^2} \text{ dB} \qquad (10)$$

or -3.92 dB.

However, a truly optimum mixer also demands that the MOSFETs exhibit an ON-state resistance of zero ohms and, of course, an ideal square-wave excitation. Neither is possible in a practical sense.

Equation (9) can be examined for various values of source and load impedances as well as r_{DS} by graphical representation, as shown in Figure 5, remembering that a nominal 3.92 dB must be added to the values obtained from the graph.

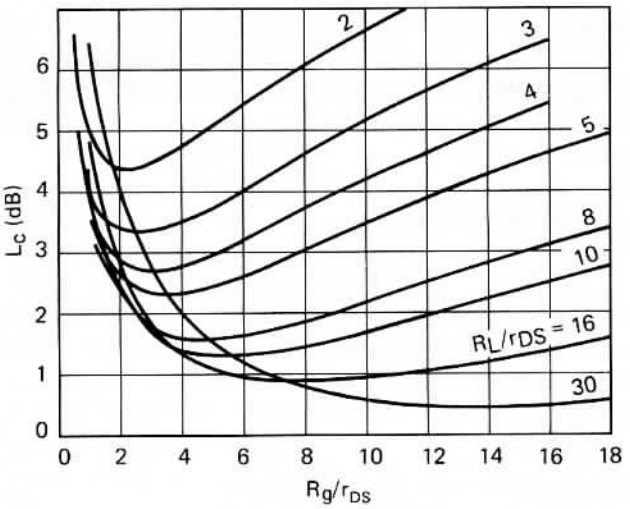

Insertion Loss As A Function of r_{DS}, R_L & R_g

Figure 5

To illustrate how seriously the ON-state resistance of the MOSFETs affects performance, we need only to consider the Si8901 with a nominal r_{DS} (at V_{GS} = 15V) of 23 ohms. With a 1:1 signal transformer (50 to 25-0-25Ω), R_g/r_{DS} = 1.1. Allowing a 4:1 IF output transformer to a 50-ohm preamplifier, the ratio R_L/r_{DS} approximates 4. From Figure 5 we read a conversion loss, L_c, of approximately 3.7 dB, to which we add 3.92 dB for a total loss of 7.62 dB. Additionally, we must also include the losses incurred by both the signal and IF transformers. The result compares favorably with measured data.

A careful study of Figure 5 reveals what appears as an anomalous characteristic. If we were to raise R_g/r_{DS} from 1.1 to 4.3 (by replacing 1:1 transformer with a 1:4 to effect a signal-source impedance of 100-0-100Ω), we would see a dramatic improvement in conversion efficiency. The anomaly is that this suggests that a mismatched signal-input port improves performance.

Caruthers (4) first suggested that reactively terminating all harmonic and parasitic frequencies would reduce the conversion loss of a ring demodulator to zero. This, of course, would also require that the active mixing elements (MOSFETs in this case) have zero r_{DS}, in keeping with the data of Figure 5.

A double-balanced mixer is a 4-port – consisting of a signal, image, IF, and local-oscillator port. Of these, the most difficult to terminate is the image frequency port simply because, in theory it exists as a separate port, but in practice it shares the signal port. Any reactive termination would, therefore, be narrow-band irrespective of its proximity to the active mixing elements.

The performance of an image-termination filter offering a true reactance to the image frequency (100% reflective) may be deduced to a reasonable degree from Figure 5, if we first presume that the conversion loss between signal and IF compares with that between signal and image. The relationship is displayed in Figure 6 where we see the expected variation in amplitude proportional to conversion efficiency (inversely proportional to conversion loss).

Image-frequency filtering affects more than conversion efficiency. As the phase of the detuned-short position of the image-frequency filter is varied, we are able to witness a cyclical variation in the intermodulation distortion as has been confirmed by measurement, shown in Figure 7. By comparing Figure 6 with Figure 7 we see that any improvement in conversion loss appears to offer a corresponding degradation in intermodulation distortion.

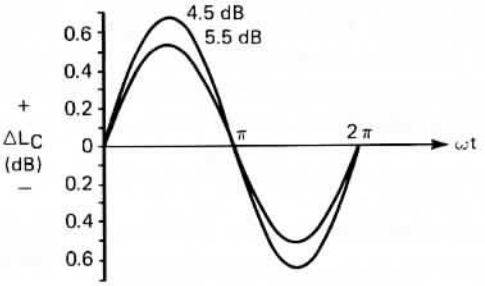

Effective of Image Termination on Conversion Loss

Figure 6

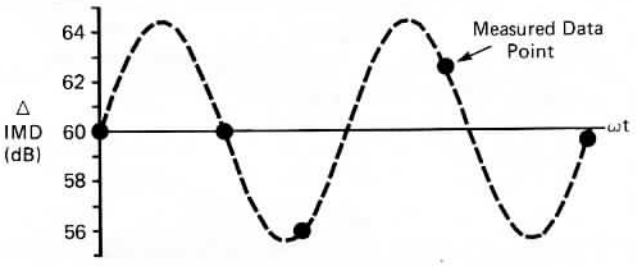

Effect of Image Termination on 3rd-Order Distortion

Figure 7

INTERMODULATION DISTORTION

Unbalanced, single-balanced, and double-balanced mixers are distinguished by their ability to selectively reject spurious frequency components, as defined in Table I. The double-balanced mixer, by virtue of its symmetry, suppresses twice the number of spurious frequencies as the single-balanced mixer suppresses.

Single-Balanced	Double-Balanced
f_s	
$3f_s$	
$5f_s$	
f1 ± f2	f1 ± f2
f1 ± 3f2	f1 ± 3f2
f1 ± 5f2	f1 ± 5f2
2f1 ± f2	
3f1 ± f2	3f1 ± f2
3f1 ± 3f2	3f1 ± 3f2
4f1 ± f2	
5f1 ± f2	5f1 ± f2

A Comparison of Modulation Products in Single and Double Balanced Mixers to the 6th Order

Table I

In the ideal mixer, the input signal is translated to an intermediate frequency without distortion, that is without impairing any of the contained information. Regrettably, the ideal mixer does not occur in practice. Because of certain non-linearities within the switching elements (MOSFETs in this case) as well as imperfect switching resulting in phase modulation, distortion results.

Identifying Intermodulation Distortion Products

The most damaging intermodulation distortion (IMD) products in receiver design are generally those attributed to odd-order and, in particular, those identified as the third-order IMD.

Any non-linear device may be represented as a power series.

$$i_d = g_m e_g + \frac{1}{2!}\frac{\delta gm}{\delta V_G} e_g^2 + \frac{1}{3!}\frac{\delta^2 gm}{\delta V_G^2} e_g^3 + \cdots \frac{1}{n!}\frac{\delta^{n-1} gm}{\delta V_G^{n-1}} e_g^n \quad (11)$$

which can be broken into

Term	Output	Transfer Characteristic
$g_m e_g$	F1, F2	Linear
$\frac{1}{2!}\frac{\delta gm}{\delta V_G} e_G^2$	2F1, 2F2 F1 ± F2	Second-Order Square-Law
$\frac{1}{3!}\frac{\delta^2 gm}{\delta V_G^2} e_G^3$	3F1, 3F2 2F1 ± F2 2F2 ± F1	Third-Order

The second-order term is the desired intermediate frequency we seek, all other higher-orders are undesirable but, unfortunately, are present to a varying degree as illustrated in Figure 8.

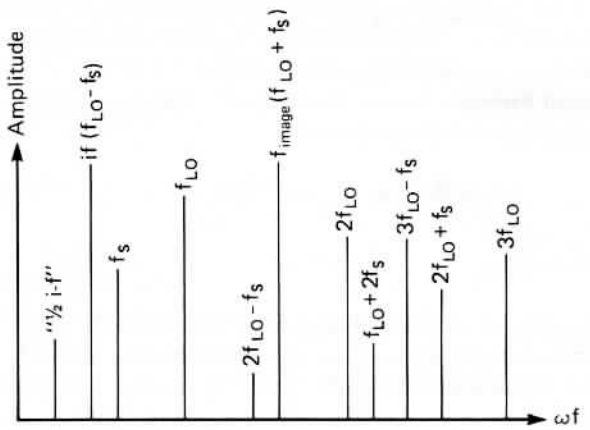

The Harmonic & Spurious Content Exiting the I-F Port of the Commutation Mixer

Figure 8

There are both fixed-level IMD products and level-dependent IMD products (5). The former are produced by the interaction between a fixed-level signal, such as the local oscillator and and the variable-amplitude signal. The resulting frequencies may be identified by

$$nf_1 \pm f_2 \quad (12)$$

where, n is an integer greater than 1.

Level-dependent IMD products result from the interaction of the harmonics of the local oscillator and those of the signal. The resulting frequencies may be identified by

$$nf_1 \pm mf_2 \quad (13)$$

where, m and n are integers greater than 1.

For a mixer to generate IMD products at the intermediate frequency, we must account for at least a two-step process. First, the generation of the harmonics of the signal and local oscillator; and second, the mixing or conversion of these frequencies to the intermediate frequency. Consequently, the mixer may be modeled as a series connection of two non-linear impedances, the first to generate the harmonic products and the second to mix or convert to the intermediate frequency. Although many harmonically-related products are possible, we will focus principally on the odd-order IMD products.

If we allow two interfering signals, f_1 and f_2, to impinge upon the first non-linear element of our mixer model, the result will be $2f_1 - f_2$ and $2f_2 - f_1$. These are identified as third-order intermodulation products (IMD_3). Other products are also generated taking the form $3f_1 - 2f_2$ and $3f_2 - 2f_1$, called fifth-order IMD products (IMD_5). Unlike the even-order products, odd order products lie close to the fundamental signals and, as a consequence, are most susceptible to falling within the passband of the intermediate frequency and thus degrading the performance of the mixer.

A qualitative definition of linearity based upon intermodulation distortion performance is called the *intercept point*. Convergence occurs when

- the fundamental output (IF) response is directly proportional to the signal input level;
- the second-order output response is proportional to the *square* of the signal input level; and,
- the third-order output response is proportional to the *cube* of the signal input level.

The point of convergence is termed the intercept point. The higher the value of this intercept point, the better the dynamic range.

Intermodulation Distortion in the Commutation Mixer

Although the double-balanced mixer outperforms the single-balanced mixer as we saw in Table I, a more serious source of intermodulation products results when the local-oscillator excitation departs from the idealized square wave (6) (7). This phenomena is easily recognized by a careful examination of Figure 9, where a sinusoidal local-oscillator voltage reacts not only upon a varying transfer characteristic but also on a varying non-linear, voltage-dependent capacitance (not shown in Figure 9). Although the effects of this sinusoidal transition are not easily derived, Ward (8) and Rafuse (9) have concluded that lowering R_g will provide improved intermodulation performance! This conflicts with low conversion loss, as we saw in Figure 5 (10), but agrees with Equation 14.

Further examination of Figure 9 reveals that the sinusoidal local-oscillator excitation results in phase modulation. That is, as the sinusoidal wave goes through a complete cycle, the resulting gate voltage, acting upon the MOSFET's transfer characteristic, produces a resulting non-linear waveform. Since all FETs have some offset – a JFET has cut-off voltage, and a MOSFET has threshold voltage – it is important, both for symmetry as well as for balance, to offer some dc offset voltage to the gates. Optimum IMD performance demands that the switches operate in a 50% duty cycle; that is, the switches must be fully ON and fully OFF for equal time. Without some form of offset bias, this would be extremely difficult unless we were to implement an idealized square-wave drive.

Walker (11) has derived an expression showing the predicted improvement in the relative level of two-tone third-order intermodulation products (IMD_3) as a function of the rise and fall times of the local-oscillator waveform.

$$20 \text{ Log } \frac{\left(t_r \omega_{LO} \frac{V_s}{V_c}\right)^2}{8} \text{ dB} \qquad (14)$$

where, V_c is the peak-to-peak local-oscillator voltage,
V_s is the peak signal voltage,
t_r is the rise and fall time of V_c,
ω_{LO} is the local-oscillator frequency.

Equation (14) offers us several interesting aspects on performance. Since any reduction in the magnitude of V_s improves the IMD, we again discover that by lowering R_g (which, in turn, decreases the magnitude of V_s) appears to benefit performance. Second, the higher the local-oscillator voltage, the better the IMD performance. Third, if we can provide the idealized square-wave drive, we achieve an infinite improvement in IMD performance!

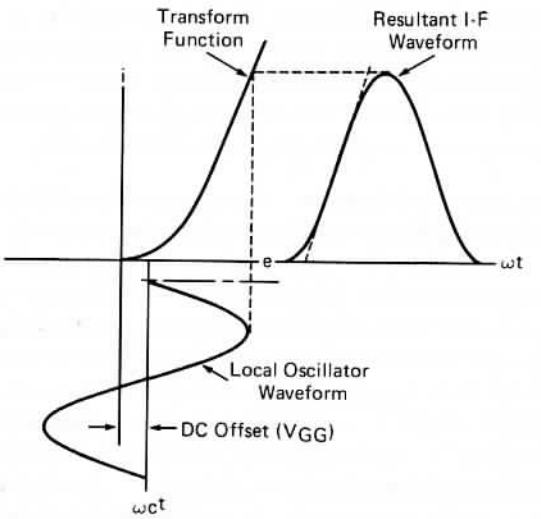

Effect of Sinusoidal L.O. Waveform on I-F Linearity

Figure 9

An additional fault of sinusoidal local-oscillator excitation results whenever the wave approaches the zero-crossing at half-period intervals. As the voltage decays, we find that any signal voltage may overload the MOSFETs causing intermodulation and crossmodulation distortion (12). This can be easily visualized from Figure 10 where we see the classic *i-e* characteristics of the MOSFET at varying gate voltages. Only at substantial gate voltage do we witness reasonable linearity and, consequently, good dynamic range.

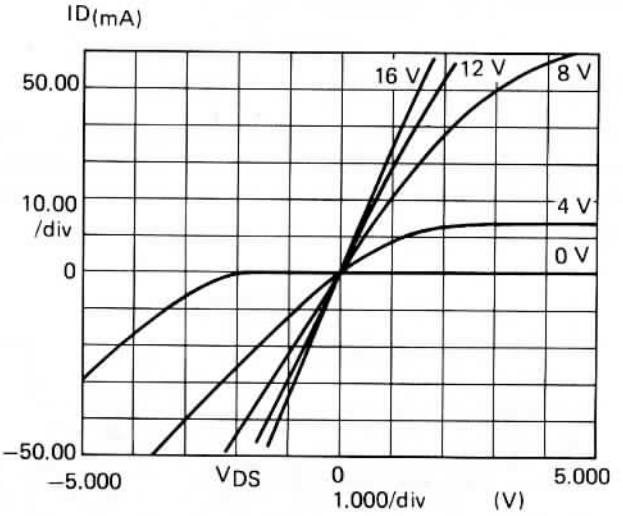

First & Third Quadrant I-E Characteristics Showing Effect of Gate Voltage Leading to Large-Signal Overload Distortion

Figure 10

DYNAMIC RANGE OF THE COMMUTATION MIXER

As the two-tone intercept point increases in magnitude, we generally expect a like improvement in dynamic range results. Yet, as we have concluded from earlier study, the intermodulation products appear to be a function of both the generator or source impedance as well as ratio R_g/r_{DS} and R_L/r_{DS} (Figure 5).

In any receiver, performance can be quantified by the term *dynamic range*. Dynamic range (DR) can be extended by improving the sensitivity to low-level signals and by increasing the power handling ability without being overcome by interfering intermodulation products or the effects caused from desensitization.

There are rules to follow if we are to improve the low-level signal sensitivity. Ideally we would like a mixer to be transparent, acting only to manipulate the incoming signals for easy processing by subsequent equipment. The perfect mixer would have no conversion loss and a low noise figure. However, in the preceeding analysis we discovered that optimum intermodulation performance occurred when the signal input port is mismatched to the quad MOSFETs (Figure 5). It now becomes clear that a performance trade-off appears necessary. Either we seek low conversion loss and with it a higher noise figure, or we aim for the highest two-tone third-order intercept point. Fortunately, as we seek the latter, our dynamic range will actually improve since a mismatched signal port has less effect upon the signal-to-noise performance of the mixer than does a matched signal port have upon intermodulation distortion.

Convention has identified minimum sensitivity to be the weaker signal which will produce an output signal that is 10 dB over that of the noise in a prescribed bandwidth (usually 1 kHz), or

$$\text{Sens.} = 20 \log \frac{V_S + V_N}{V_N} + 10\,\text{dB} \qquad (15)$$

Desensitization occurs whenever a nearby unwanted signal causes the compression of the desired signal. The effect appears as an increase in the mixer's conversion loss.

THE Si8901 AS A COMMUTATION MIXER

Because of package and parasitic constraints, the Si8901 is best suited for performance in the HF to low VHF region. A surface-mount version may extend performance to somewhat higher frequencies.

In our review of intermodulation distortion, we recognized that to achieve a high intercept point the local-oscillator drive must

- approach the ideal square-wave,
- ensure a 50% duty cycle,
- offer sufficient amplitude to ensure a full ON and OFF switching condition, as well as to offer reduced r_{DS} when ON.

Furthermore, to maintain superior overall performance – both in conversion loss, dynamic range (noise figure) and intercept point – some form of image-frequency termination would be highly desirable even though, understandably, the mixer's bandwidth would be restricted.

Consequently, the principal effort in the design of a high dynamic range commutation mixer is two-fold. First, and most crucial, is to achieve a gating or control voltage sufficient to ensure a positive and hard turn-ON as well as a complete turn-OFF of the mixing elements (MOSFETs). Second, and of lesser importance, is to properly terminate the parasitic and harmonic frequencies developed by the mixer.

Establishing the Gating Voltage

Local oscillator injection to the conventional diode ring, FET, or MOSFET double-balanced mixer is by the use of the broadband, transmission-line transformer (13), as shown in Figure 11. For the diode-ring mixer where switching is a function of loop current, or for active FET mixers that operate on the principle of transconductance and thus need little gate voltage (14), the broadband transformer is adequate. If this approach is used for the commutation mixer, we would need extraordinarily high local-oscillator drive to ensure positive turn-ON. Rafuse (15) and Ward (16) used a minimum of 2 W to ensure mixing action; Lewis and Palmer (17) achieved high dynamic range using 5 Watts! The MOSFETs used in these early designs were p-channel, enhancement-mode (2N4268) devices with moderately high threshold (6 V maximum) and high input capacity (6 pF maximum). All of these early MOSFET double-balanced mixers relied on the conventional 50 to 100-0-100-Ω transformer for local-oscillator injection to the gates.

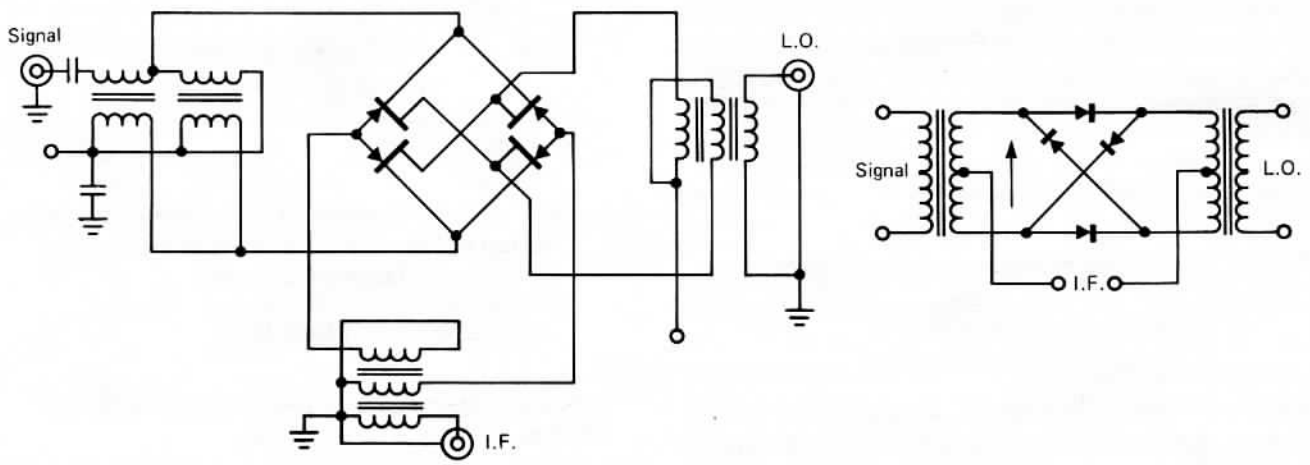

Local Oscillator Drive Using Conventional Broadband Transformers

Figure 11

A major goal is the conservation of power. This goal cannot be achieved using the conventional design. Simply increasing the turns ratio of the coupling transformer is thwarted by the reactive load presented by the gates.

The obvious solution is to use a resonant gate drive. The voltage appearing across the resonant task – and thus on the gates – may easily be calculated,

$$V = (P \cdot Q \cdot X)^{1/2} \quad (16)$$

where, P is the power delivered to the resonant tank circuit,

Q is the *loaded* Q of the tank circuit, and

X is the reactance of the gate capacity.

Since the gate capacitance of the MOSFET is voltage dependent, the reactance of the gate becomes dependent upon the impressed excitation voltage. To allow this would severely degrade the IMD performance of the mixer. However, we can minimize the change in gate capacitance and remove its detrimental influence using a combination of substrate and gate bias, as shown in Figure 12. Not only does this show itself beneficial in this regard, but as we saw in Figure 9, a gate bias is necessary to ensure the required 50% duty cycle. Furthermore, a negative substrate voltage ensures that each MOSFET on the monolithic substrate is electrically isolated and that each source-/drain-to-body diode is sufficiently reverse biased to prevent half-wave conduction.

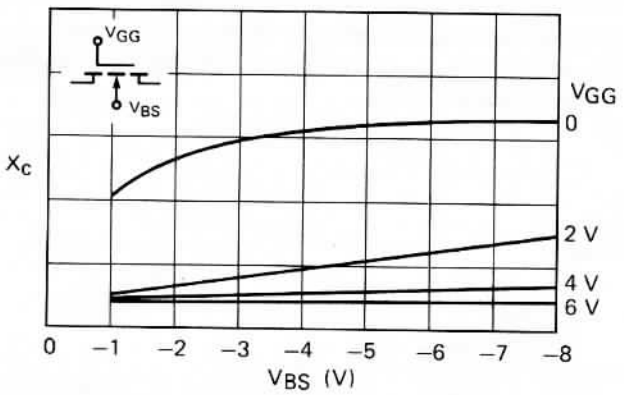

Effect of Bias on Gate Reactance

Figure 12

Implementing the resonant gate drive may take any of several forms. The resonant tank circuit may be merged with the oscillator, or it can be a varactor-tuned Class B stage (18), or as in the present design, an independent resonant tank, shown in Figure 13.

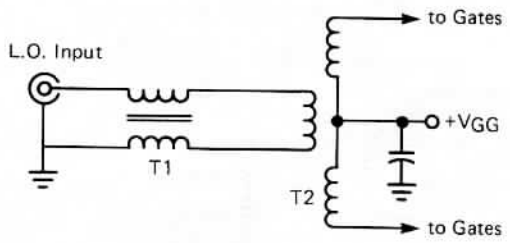

Resonant - Gate Drive. T2 is Tuned to Resonate with C_{gs} of Si8901

Figure 13

To ensure symmetrical gate voltage in 180-degree anti-phase, if the local-oscillator drive is asymmetrical, i.e., fed by unbalanced coax, an unbalanced-to-balanced balun must be used (T1 in Figure 13); otherwise, capacitive unbalance results with an attendant loss in mixer performance.

Table II offers an interesting comparison between a resonant-gate drive with a loaded tank Q of 14 and a conventional gate drive using a 50 to 100-0-100-Ω transformer. The importance of a high tank Q is graphically portrayed in Figure 14. The full impact of a high gate voltage swing can be appreciated by using Equation (14). Here, as V_c (gate voltage) increases the intermodulation performance (IMD) also improves, as we might intuitively expect. Calculated and measured results are shown in Figure 15 and demonstrate reasonable agreement. The difference may reflect problems encountered in measuring V_c as any probe will inadvertently load, or detune, the resonant tank even with the special care that was taken to compensate.

Power in (mW)	NR Gate Voltage (V)	Res Gate Voltage (V)
10	0.20	5.4
20	0.29	7.7
30	0.33	9.4
60	0.44	13.3

Comparision of a-c gate voltage versus local-oscillator drive between a non-resonant (NR) and resonant (Res) tank with a loaded Q of 14 (Freq. 150 MHz)

Table II

If we have the option to choose "high side" or "low side" injection – i.e., having the local-oscillator frequency above (high) or below (low) the signal frequency – a closer inspection of Equation (14) should convince us to choose low-side injection.

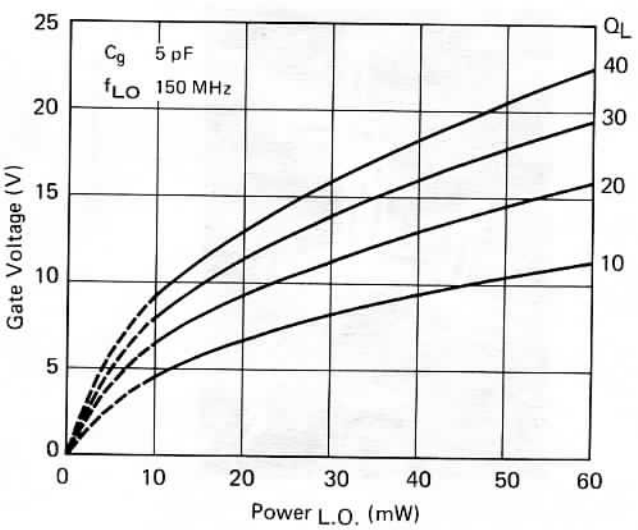

Influence of Loaded Q on Gate Voltage vs L.O. Power

Figure 14

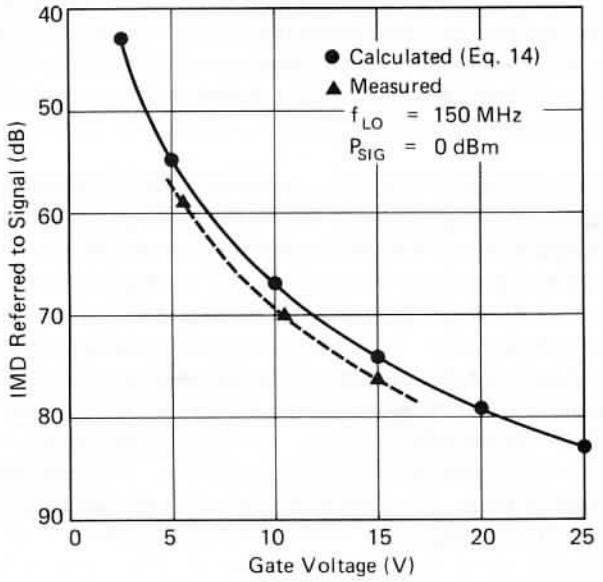

Effect of Gate Voltage on IMD Performance

Figure 15

Terminating Unwanted Frequencies

If our mixer is to be operated over a restricted frequency range where the local oscillator and signal frequencies can be manipulated, image-frequency filtering may be possible. Image-frequency filtering does affect performance – for high-side local-oscillator injection, an elliptic-function low-pass filter, or for low-side injection, a high-pass filter might offer worthwhile improvement. In either case, the filter offers a short-circuit reactance to the image frequency forcing the image to return once again for demodulation. The results of using a low-pass filter with the prototype commutation mixer are known from our earlier examination of Figures 6 and 7.

The resonant-gate drive consisting of a high-Q tank offers adequate bypassing of the intermediate frequency and image frequency.

If the IF port is narrow band, filtering may be possible by simply using a resonant L-C network across the primary of the transformer (19).

Design Techniques in Building the Mixer

The mixer was fabricated on a high-quality double-copper clad board shown in Figure 16. An improvised socket held the Si8901.

The signal and IF ports used Mini-Circuits, Inc., plastic T-case RF transformers. For the intermediate frequency, the Mini-Circuits T4-1 (1:4) was used; for the signal, the Mini-Circuits T1-1T (1:1) or T4-1 was used. The resonant tank was wound on a one-quarter-inch-diameter ceramic form with no slug. The unbalanced-to-balanced resonant tank drive used a T4-1. The schematic diagram, Figure 17, is for a commutation mixer with high-side injection, operating with an IF of 60 MHz.

The principle effort involved the design of the resonant-gate drive. This necessitated an accurate knowledge of the gate's total capacitive loading effect. To accomplish this, a precision fixed capacitor (5 pF) was substituted for the Si8901, and at resonance, it was a simple matter to calculate the inductance of the resonant tank. Substituting the Si8901 made it again a simple task to determine the capacitive effects of the Si8901. Once known, a high-Q resonant tank can be quickly designed and implemented. To ensure good interport isolation, symmetry is important, so care is necessary in assembly to maintain mechanical symmetry, especially with the primary winding.

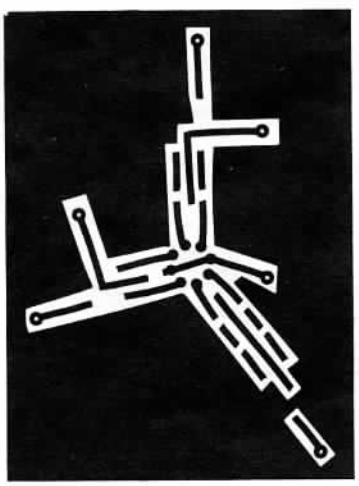

Mask Layout PCM Prototype Commutation Mixer

Figure 16

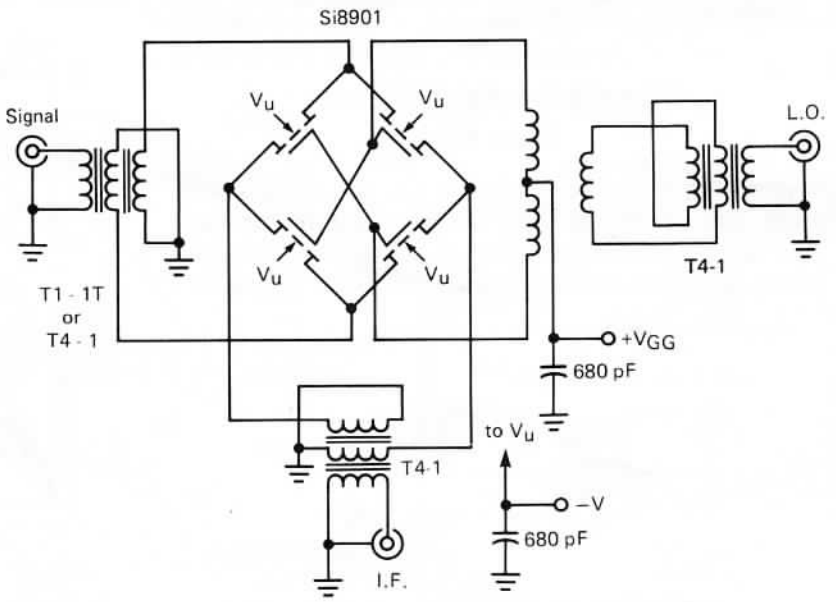

Prototype Commutation Double-Balanced Mixer

Figure 17

Performance of the Si8901 Prototype Commutation Mixer

The primary goal in developing a commutation double-balanced mixer is to achieve a wide dynamic range. If this task can be accomplished with an attendant savings in power consumption, then the resulting mixer design should find wide application in HF receiver design.

The following tests were performed.

- conversion efficiency (loss)
- two-tone, 3rd order intercept point
- compression level
- desensitization level
- noise figure

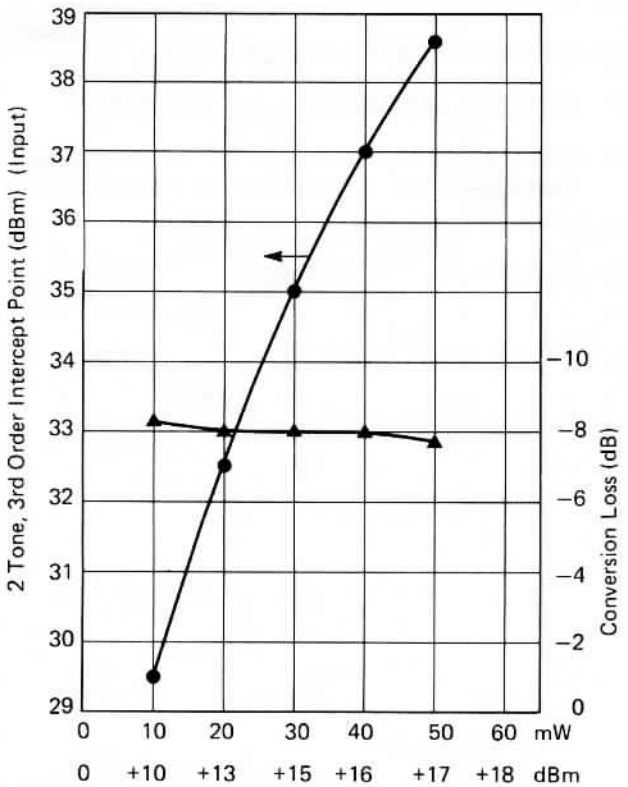

Intercept Point & Conversion Loss

Figure 18

Conversion loss and the intercept point are directly dependent upon the magnitude of the local-oscillator power. The prototype mixer's performance is offered in Figure 18, where the *input* intercept is plotted.

Both the compression and desensitization levels may appear to contradict reason. Heretofore, conventional diode-ring demodulators exhibited compression and desensitization levels an order of magnitude *below* the local-oscillator power level. However, with a commutation MOSFET mixer, switching is *not* accomplished by the injection of loop current but by the application of gate *voltage*. At a local-oscillator power level of + 17 dBm (50 mW), the 2 dB compression level and desensitization level was + 30 dBm!

The single-sideband HF noise figure of 7.95 dB was measured at a local oscillator power level of + 17 dBm.

CONCLUSIONS

Achieving a high gate voltage to effect high-level switching by means of a resonant tank is not a handicap. Although one might, at first, label the mixer as narrow-band, in truth the mixer is wideband. For the majority of applications, the intermediate frequency is fixed, that is, narrow band. Consequently, to receive a wide range of signal frequencies, the local oscillator is tuned across a similar band. In modern technology the tuning can be accomplished by numerous methods, not the least of which might be electronically using varactors. The resonant tank also may take several forms. It can be part of the oscillator, or as in Reference (18), it can be varactor-tuned driver electronically tracking the local oscillator.

If the local-oscillator drive was processed to offer a more rectangular waveform, approaching the idealized square wave, we might then anticipate even greater dynamic range as predicted by Equation (14).

REFERENCES

1. Oxner, Ed., "Fets Work Well in Active Balanced Mixers," *EDN*, Vol. 18, No. 1 (January 5, 1973), pp. 66-72.

2. Oxner, Ed., "Active Double-Balanced Mixers Made Easy With Junction FET's," *EDN*, Vol. 19, No. 13 (July 5, 1974), pp. 47-53.

3. Walker, H.P., "Sources of Intermodulation in Diode-Ring Mixers," *The Radio and Electronic Engineer*, Vol. 46, No. 5 (May 1967), pp. 247-255.

4. Caruthers, R.S., "Copper Oxide Modulators in Carrier Telephone Repeaters," *Bell System Technical Journal*, Vol. 18, No. 2 (April 1939), pp. 315-337.

5. Mouw, R.B., & S.M. Fukuchi, "Broadband Double Balanced Mixer/Modulators," *Microwave Journal*, Vol. 12, No. 3 (March 1969), pp. 131-134.

6. Lewis, H.D., & F.I. Palmer, "A High Performance HF Receiver," R.C.A. Missiles & Surface Radar Division Report (November 1968).

7. Walker, H.P., *op. cit.*

8. Ward, Michael John, "A Wide Dynamic Range Single-Sideband Receiver," M.I.T. *MS Thesis*, (December 1968).

9. Rafuse, R.P., "Symmetric MOSFET Mixers of High Dynamic Range," *Digest of Technical Papers*, 1968 Int'l Solid-State Circuits Conf., pp. 122-123.

10. Lewis, H.D., & F.I. Palmer, *op. cit.*, pg. 13.

11. Walker, H.P., *op. cit.*

12. Gardiner, John G., "The Relationship Between Cross-Modulation and Intermodulation Distortions in the Double-Balanced Modulator," IEEE Proc. *Letters* (November 1968), pp. 2069-2071.

13. Ruthroff, C.L., "Some Broad-Band Transformers," *Proc. IRE* (August 1959), pp. 1337-1342.

14. Kwok, Siang-Ping, "A Unified Approach to Optimum FET Mixer Design," Motorola Application Note AN-410 (n.d.)

15. Rafuse, R.P., *op. cit.*

16. Ward, Michael John, *op. cit.*, pg. 55.

17. Lewis, H.D., & F.I. Palmer, *op. cit.*, Table 1, pg. 26.

18. "Electronically Controlled High Dynamic Range Tuner," *Final Report* (June 1971) ECOM-0104-4 Research and Development Technical Report, AD887063L.

19. *ibid.*